

# Lawrence Berkeley National Laboratory

## Lawrence Berkeley National Laboratory

### **Title**

Model for I/f Flux Noise in SQUIDs and Qubits

### **Permalink**

<https://escholarship.org/uc/item/6401n5gc>

### **Authors**

Koch, Roger H.  
DiVincenzo, David P.  
Clarke, John

### **Publication Date**

2007-01-19

Peer reviewed

## **Model for $1/f$ Flux Noise in SQUIDs and Qubits**

*Roger H. Koch,<sup>1</sup> David P. DiVincenzo<sup>1</sup> and John Clarke<sup>2</sup>*

*<sup>1</sup>IBM Research Division, Thomas J. Watson Research Center, Yorktown Heights, NY 10598*

*<sup>2</sup>Department of Physics, University of California, Berkeley, CA 94720-7300 and  
Materials Sciences Division, Lawrence Berkeley National Laboratory, Berkeley CA 94720*

(Dated: January 19, 2007)

We propose a model for  $1/f$  flux noise in superconducting devices ( $f$  is frequency). The noise is generated by the magnetic moments of electrons in defect states which they occupy for a wide distribution of times before escaping. A trapped electron occupies one of the two Kramers-degenerate ground states, between which the transition rate is negligible at low temperature. As a result, the magnetic moment orientation is locked. Simulations of the noise produced by a plausible density of randomly oriented defects yield  $1/f$  noise magnitudes in good agreement with experiments.

PACS numbers: 03.67.Lx, 05.40.Ca, 85.25.Dq

The phenomenon of  $1/f$  noise, with spectral density  $S(f)$  scaling inversely with frequency  $f$ , is common to virtually all devices. In 1983, Koch *et al.* [1] identified two separate sources of  $1/f$  noise in dc SQUIDs (Superconducting QUantum Interference Devices): critical current noise and flux noise. The  $1/f$  flux noise  $S_\Phi^{1/2}$  (1 Hz) was within a factor of 3 of  $10 \mu\Phi_0 \text{ Hz}^{-1/2}$  for Nb- or Pb-based SQUIDs at 4.2 K, even though the loop areas ranged over 6 orders of magnitude; here,  $\Phi$  denotes magnetic flux and  $\Phi_0 \equiv h/2e$  is the flux quantum. Subsequently, other authors found rather lower levels of  $1/f$  flux noise at 1 Hz and 4.2 K, for example,  $0.5 \mu\Phi_0 \text{ Hz}^{-1/2}$  [2] and  $0.2 \mu\Phi_0 \text{ Hz}^{-1/2}$  [3]. Wellstood *et al.* [4] reported values of  $S_\Phi^{1/2}$  (1 Hz) of  $(4-10) \mu\Phi_0 \text{ Hz}^{-1/2}$  at temperatures below 0.1 K in 12 Nb, Pb and PbIn devices. Recently, Nakamura *et al.* [5] showed that  $1/f$  flux noise with  $S_\Phi^{1/2}$  (1 Hz)  $\approx 1 \mu\Phi_0 \text{ Hz}^{-1/2}$  determined the decoherence time in their Al-based flux qubits at 20 mK. The value of  $S_\Phi^{1/2}$  (1 Hz) in the SQUIDs of Wellstood *et al.*, with areas up to  $2 \times 10^5 \mu\text{m}^2$ , is at most one order of magnitude higher than that in these qubits, with an area of about  $3 \mu\text{m}^2$ , five orders of magnitude less. These results, and that of Ref. 1, rule out the notion of a “global magnetic field noise”.

Critical current fluctuations in Josephson junctions have been widely studied, for example [6-8], and are understood to arise from the trapping and release of electrons in traps in the tunnel barrier. In the case of high transition temperatures ( $T_c$ ) SQUIDs at 77 K,  $1/f$  flux noise is ascribed to thermal activation of vortices among pinning sites [9]. This noise can be eliminated by reducing the linewidth to below  $(\Phi_0/B)^{1/2}$ , thereby making it energetically unfavorable for the film to trap a vortex [10];  $B$  is the magnetic field in which the device is cooled. Given that the low- $T_c$  devices are made of films with a much higher pinning energy, are operated at much lower temperatures, and may have linewidths orders of magnitude less

than  $(\Phi_0/B)^{1/2}$ , vortex motion is not a viable mechanism for their  $1/f$  flux noise. We can also rule out nuclear spins as the origin of flux noise: the nuclear moment density in the SQUIDs and their substrates is simply not large enough to account for the observed magnitude of this noise. Thus, the origin of  $1/f$  flux noise in low- $T_c$  devices—despite its ubiquitous nature and the limitations it imposes on SQUIDs and qubits alike—has remained an unsolved puzzle.

In this paper, we propose a model for  $1/f$  flux noise in low- $T_c$  devices. Our basic assumption is that the noise is generated by unpaired electrons that hop on and off defect centers by thermal activation. The spin of an electron is locked in direction while the electron occupies a given trap; this direction varies randomly from trap to trap. The relevant trapping energies have a broad distribution on the scale of  $k_B T$  [11], so that the characteristic times over which an electron resides on any one defect vary over many orders of magnitude. The uncorrelated changes of these spin directions yield a series of random telegraph signals that sum to a  $1/f$  power spectrum [12]. There is no shortage of candidates for microscopic defect centers involved in this process: In amorphous  $\text{SiO}_2$ , these include  $E'$  center variants, in which an electron is captured by a silicon atom that has an oxygen vacancy, the nonbridging oxygen hole center (NBOHC) where a hole is trapped on an oxygen atom that has only one bond with the lattice, and the superoxide radical, in which a hole is trapped on an additional oxygen atom [13]. In addition, although not nearly as extensively studied as  $\text{SiO}_2$ , the amorphous oxides of superconductors such as  $\text{AlO}_x$  and  $\text{NbO}_x$  contain large densities of defects of various sorts: for example, the concentration of OH defects in  $\text{AlO}_x$  can reach several percent [14, 15].

Elucidation of this model involves two key steps. First one has to understand how the direction of an electron spin can remain fixed for very long periods of time—longer than the

inverse of the lowest frequency at which the  $1/f$  noise is observed, say,  $10^{-4}$  Hz. Second, one has to calculate the net fluctuating flux coupled into a superconducting loop. We address these two issues in turn.

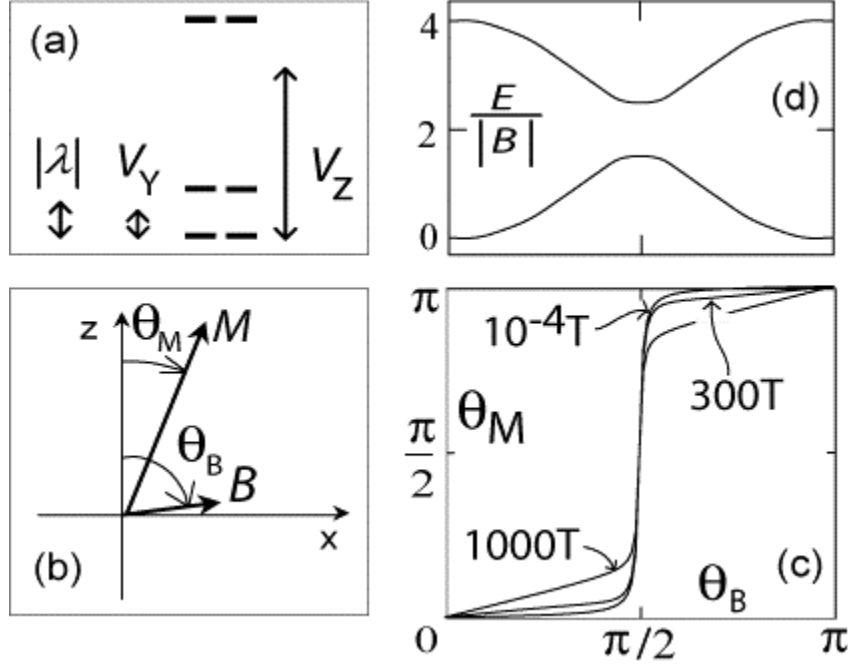


FIG. 1(a). Properties of the p-orbital defect model, Eq. (1). We take crystal-field parameters  $V_x = 0$ ,  $V_y = 400K$ ,  $V_z = 2000K$ , and spin-orbit coupling  $\lambda = -600K$ . (a) The six energy levels of the model. The levels do not carry definite angular momentum quantum numbers, but occur in Kramers-degenerate pairs, no matter how strong the spin-orbit coupling. The mixing of the lowest four levels when  $|\lambda|$  is comparable to the crystal field parameters  $V_{y,z}$  results in a locking of the magnetic moment direction; this locking is not present if  $|\lambda| \gg V_{y,z}$  or if  $|\lambda| \ll V_{y,z}$ . (b) The idea of locking: even if the applied field  $B$  is at a large angle  $\theta_B$  from the principal axis  $z$  of the crystal field, the resultant magnetization vector  $M$  lies at a small angle  $\theta_M$  from  $z$ . (c) The calculated  $\theta_M$  vs.  $\theta_B$  for  $|B| = 10^{-4} T$ ,  $300 T$ , and  $1000 T$ . For a defect with these parameters, locking is strong for any practical field; it remains strong up to near  $1000 T$ , when the magnetic energy in Eq. (1) becomes comparable to the crystal-field and spin-orbit energies.  $M$

unlocks as  $\theta_B$  passes through  $\frac{\pi}{2}$ , rotating rapidly to the opposite direction; however, if  $\frac{E}{|\mathbf{B}|}$  is large enough, this rapid rotation is prevented due to a Landau-Zener tunneling between the first and second energy levels. (d) The anticrossing of these levels near  $\theta_B = \pi/2$ ;  $\frac{E}{|\mathbf{B}|}$  is in units of  $\mu_B$ . The anticrossing gap scales with  $|\mathbf{B}|$ , so that this Landau-Zener tunneling will occur readily at low fields.

Our key assumption is that an electron randomly adopts a low-energy spin direction when it arrives at a defect, and that it remains *locked* in that orientation during its entire residence time. If the magnetic field  $\mathbf{B}$  is zero, Kramers' theorem [16] guarantees that the ground state is doubly degenerate, the two states having oppositely directed angular momenta [Fig. 1(a)]. It is well known that scattering mechanisms that take the electron from one member of the doublet to the other are extremely weak: the “Van Vleck cancellation” [17] implies that direct phonon scattering is forbidden. Higher order processes are allowed, but those that have been studied are strongly suppressed at low temperature; for example, the phonon Raman scattering rate [18] has a temperature dependence of  $T^{13}$ .

Of course, the magnetic field is not strictly zero; any particular defect experiences fluctuating dipole fields from neighboring defects of the order of  $10^{-4}$  T (root mean square). But the magnetic-moment direction of the defect is stable also with respect to these fluctuations. This magnetic moment vector  $\hat{\mathbf{M}} = \mu_B (\hat{\mathbf{L}} + 2\hat{\mathbf{S}})$  can be locked as a result of spin-orbit coupling. The following model Hamiltonian [19] provides a good generic description of this locking effect:

$$\hat{H} = \sum_{i=x,y,z} V_i |p_i\rangle\langle p_i| + \lambda \hat{\mathbf{L}} \cdot \hat{\mathbf{S}} + \mu_B \mathbf{B} \cdot (\hat{\mathbf{L}} + 2\hat{\mathbf{S}}). \quad (1)$$

In this model, the unpaired electron occupies a p-orbital; the  $V_{x,y,z}$  are the matrix elements of the crystal field potential (there will be a preferred coordinate system, varying randomly from

defect to defect, for which the crystal-field tensor is diagonal, as shown). The spin-orbit coupling constant  $\lambda$  is observed to have a large range of possible magnitudes for different defects, in the range of 10 K to 5000 K, but for defects involving atomic weights near that of silicon,  $|\lambda| \approx 300K$  is typical. The scale of the crystal field parameters  $V_{x,y,z}$  is set by chemical energies, and so can range up to  $\approx 2000K$ . It is often said that the orbital angular momentum of simple defects is “quenched” [20], meaning that  $\langle \hat{\mathbf{L}} \rangle = \mathbf{0}$  and that the magnetic moment arises only from the (unlocked) spin angular momentum. Equation (1) exhibits this behavior if  $|V_i - V_j| \gg |\lambda|$  ( $i \neq j = x,y,z$ ). But, it seems quite reasonable that there is a substantial subpopulation of defects for which  $|V_i - V_j| \approx |\lambda|$ , and for these Figs. 1(b) and (c) show that the direction of  $\mathbf{M} = \langle \Psi_\theta | \hat{\mathbf{M}} | \Psi_\theta \rangle$  for the ground state  $|\Psi_\theta\rangle$  is very stable with respect to variations in the direction of a  $10^{-4}$ -T magnetic field, being locked to the principal axis of the crystal field. In defects for which  $\lambda < 0$ ,  $\mathbf{L}$  and  $\mathbf{S}$  are parallel and  $\mathbf{M}$  is large, while for the  $\lambda > 0$  defects,  $\mathbf{M}$  is near zero (i.e., the anisotropic Lande g-factor is near zero) because  $\mathbf{L}$  and  $\mathbf{S}$  are antiparallel; thus, we expect the  $\lambda < 0$  subpopulation to be most important for flux noise.

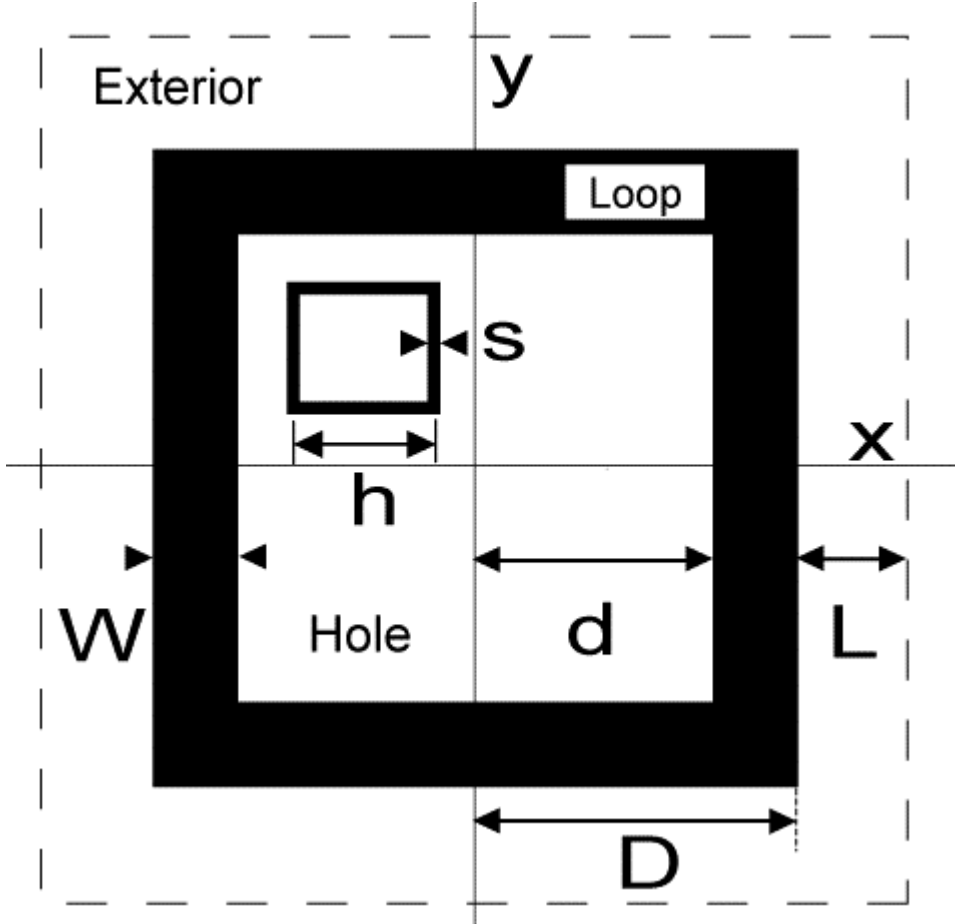


FIG. 2 Configuration of SQUID loop and test loop representing a perpendicular magnetic moment.

Given this picture of the underlying physical processes, we now calculate the flux noise coupled into a SQUID or qubit (henceforth succinctly referred to as “SQUID”) by a spatially random distribution of electron spins fluctuating in orientation. We assume—for lack of more specific information—that the defects are randomly distributed over the substrate, everywhere with the same areal density  $n$ . We consider three regions that produce noise (Fig. 2): the hole of the SQUID (“hole noise”), the region outside the SQUID



(“exterior noise”) and the loop itself (“loop noise”) [21]. For purposes of simulating the coupling between an electron magnetic moment and the SQUID, we represent the moment by a small test current loop (Fig. 2). The SQUID loop lies in the plane  $z = 1\mu\text{m}$ , has inner and outer dimensions of  $2d$  and  $2D$ , and a thickness of  $0.1\mu\text{m}$ . To simulate the random orientation of the magnetic moment, it suffices to add contributions from the three coordinate directions. For most purposes we will need only a current loop in the plane  $z = 0$  (“perpendicular (p) moment” – see Fig. 2) or in the plane  $x = 0$  (“in-plane (i) moment”). The test loop has an effective area  $A = h^2 = (0.1\mu\text{m})^2$ , a strip width  $s = 0.03\mu\text{m}$ , a thickness of  $0.1\mu\text{m}$ , and carries a current  $i$  chosen so that  $Ai = \mu_B$ , where  $\mu_B = 9.27 \times 10^{-24} \text{JT}^{-1}$  is the Bohr magneton (the scale of the magnetic moment of the defects modeled above). For the test loop at a specified location, we compute its mutual inductances  $M_p$  and  $M_i$  with the SQUID loop using the superconducting version of FastHenry [22]. The flux coupled into the SQUID for a single electron moment is given by  $\Phi_s = M(x,y)i = M(x,y)\mu_B/A$ . We will study the quantity  $\phi_s/\mu_B = \Phi_s/\Phi_0\mu_B = M(x,y)/A\Phi_0$ —the flux (in units of  $\Phi_0$ ) per Bohr magneton coupled into the SQUID loop.

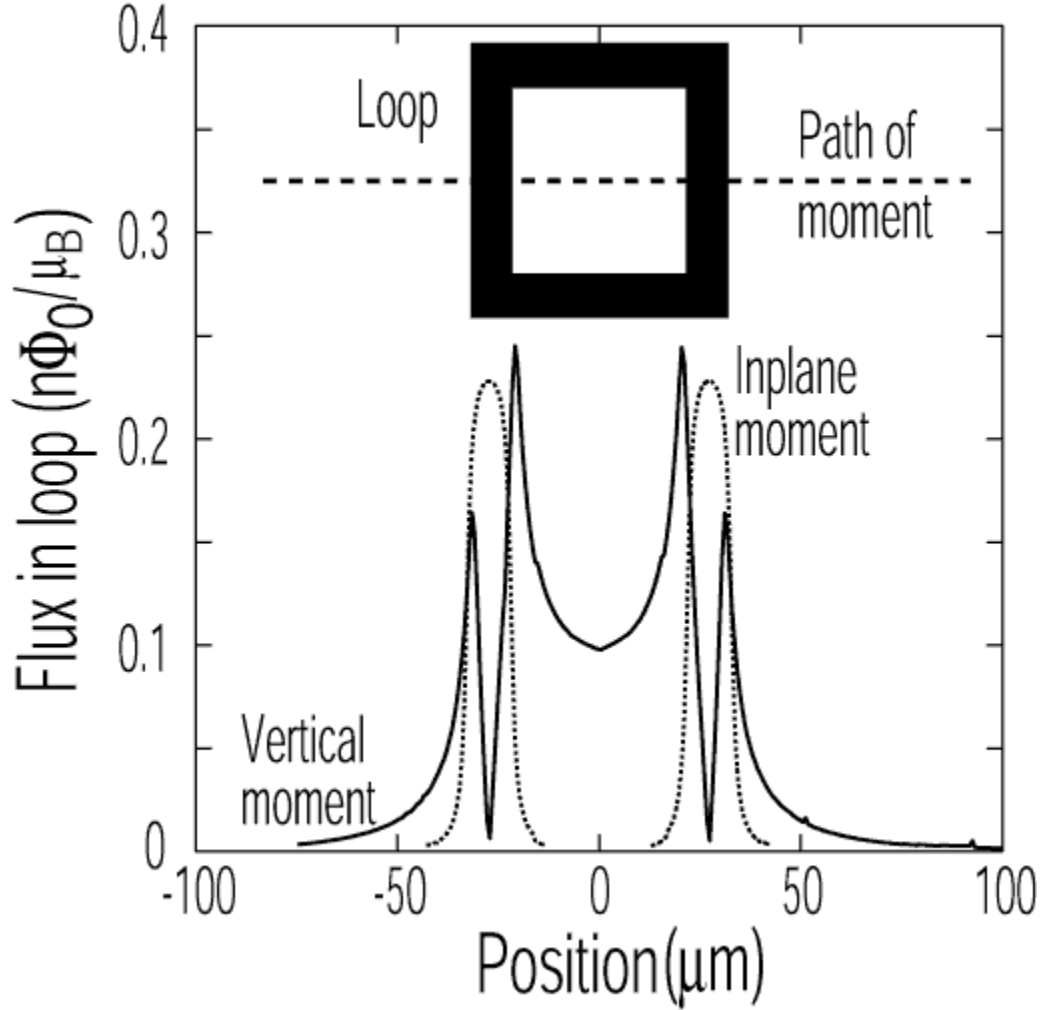


FIG. 3 Flux in units of  $\phi_s/\mu_B$  coupled to SQUID loop by a current loop moved along the line indicated. “In plane” and “perpendicular” refer to the orientation of the magnetic moment. SQUID dimensions are  $2D = 52 \mu\text{m}$  and  $2d = 41.6 \mu\text{m}$ .

In Fig. 3 we plot  $\phi_s(x,y)/\mu_B$  as a function of  $x$  for constant  $y$  for the magnetic moment perpendicular to the plane and in plane. As expected, the plots are symmetric about the origin. For the perpendicular moment,  $\phi_s(x,y)$  has a local minimum at the center, and increases towards either edge of the superconductor. When the moment is at the midpoint under (or over) the superconducting film, the coupled flux is essentially zero as expected from symmetry. The flux coupled into the SQUID loop from an exterior moment also peaks

at the edges of the superconductor. For the in-plane moment,  $\phi_s(x,y)$  peaks at the midpoints of the superconducting film, and falls off rapidly as the moment moves away from the film. By symmetry, away from the superconducting region the flux would be zero if the moment and the SQUID loop were in the same plane.

To obtain the noise due to an ensemble of spins, we first integrate  $M_p$  or  $M_i$  over an element  $ydx$  in one quadrant . The range of integration extends to a distance  $L = 100 \mu\text{m}$  beyond the outer edge of the SQUID, where  $M_p$  or  $M_i$  is two orders of magnitude less than at  $(0,0)$ . For either case, the total mean square normalized flux noise coupled into the SQUID, summed over the hole, superconductor and exterior contributions, is given by

$$\langle(\delta\phi_s)^2\rangle = 8n\mu_B^2 \int_0^{(D+L)} [M(x,y)/\Phi_0 A]^2 y dx . \quad (2)$$

To convert the mean square flux noise to a spectral density  $S_\Phi(f) = \alpha/f$ , where  $\alpha$  is a constant, we introduce lower and upper cut-off frequencies,  $f_1$  and  $f_2$ , and set  $\langle(\delta\Phi_s)^2\rangle = \alpha \int_{f_1}^{f_2} df/f = \alpha \ln(f_2/f_1)$ . Taking the rough values  $f_1 = 10^{-4}$  Hz and  $f_2 = 10^9$  Hz (the results are only weakly sensitive to these values), we find  $S_\Phi(f)/\Phi_0^2 \approx \langle(\delta\Phi_s/\Phi_0)^2\rangle/30f$ . To find the total noise from an ensemble of spins with uniformly distributed orientations we calculate  $\langle M^2 \rangle$ , which we insert into Eq. (2).

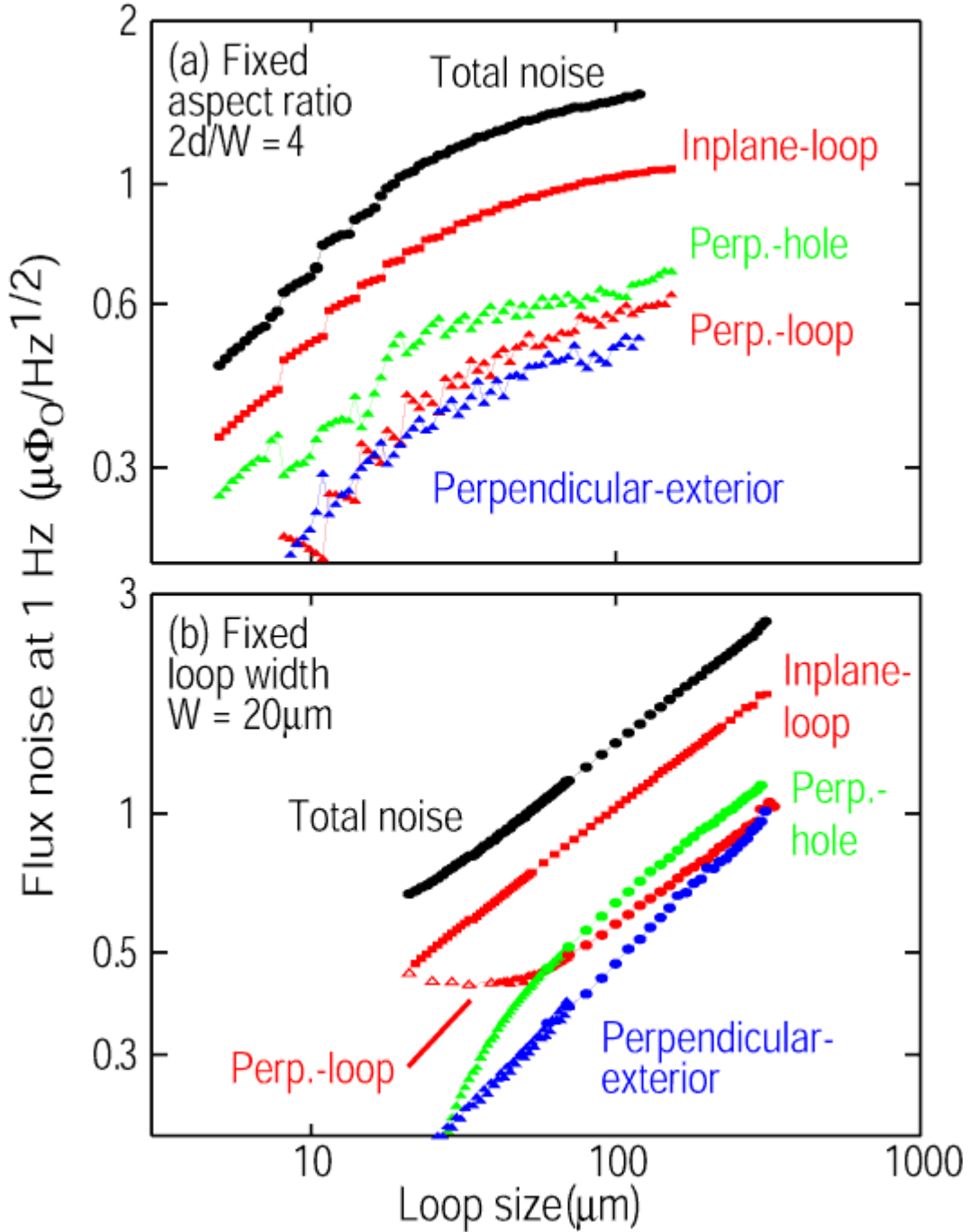


FIG. 4 Computed flux noise versus loop size  $D + d$  for (a) fixed loop aspect ratio  $2d/W = 4$  and (b) fixed width  $W = 20 \mu\text{m}$ . The jagged behavior in (a) is due to the discrete mesh of FastHenry. The open triangles in (b) indicate that the accuracy of the calculations is of limited accuracy.

We plot the normalized amplitude spectra of the flux noise in the SQUID at 1 Hz,  $S_{\Phi}^{1/2}(1 \text{ Hz})/\Phi_0$ , in Fig. 4. We assume a defect density  $n$  of  $5 \times 10^{17} \text{ m}^{-2}$ . Figure 4(a) shows the contributions of the hole, loop and exterior noises for the perpendicular moments, the loop noise for the in plane moments and the total noise versus the mean loop size  $D + d$  for constant aspect ratio  $2d/W$ . All the contributions follow the same general trend, increasing by a factor of 4 when the loop area is increased by a factor of about 200. Figure 4(b) shows the same noise contributions versus  $(D + d)$  for fixed  $W$ . As expected, the hole noise vanishes as the area of the hole vanishes. At values of  $(D + d)$  greater than about  $50 \mu\text{m}$ , the slope tends asymptotically to 0.5. This result implies that  $S_{\Phi}(1 \text{ Hz})$  scales with the linear dimension of the SQUID, that is, with the perimeter rather than the area. Thus, once the dimensions of the hole exceed the strip width, the noise is dominated by defects relatively close to or underneath (or on top of) the superconductor, and the contributions from the central region of the loop become unimportant. The total noise ranges from about 0.7 to  $2.5 \mu\Phi_0 \text{ Hz}^{-1/2}$  over the range shown. This magnitude is of course dictated by our estimated value of  $n$ .

We also considered the noise generated when electrons hop between two spatially separated traps while maintaining the same orientation of  $\mathbf{M}$ , for example, on the surface of an insulator with no nearby metal. We find that an electron would have to move a distance of approximately  $5 \mu\text{m}$  to reproduce the flux change in the loop that results from an occupation change of one electron in a trap at the same location. Since the mean distance between traps is much less than  $5 \mu\text{m}$ , and the orientation of  $\mathbf{M}$  will on average change when moving from trap to trap, we neglect the contributions of such “translational noise” compared

with the “occupational noise”, discussed above, produced by the uncorrelated filling and emptying of isolated traps.

In summary, we have shown that flux noise in superconducting devices can be explained in terms of electrons that hop between traps in which their spins have fixed, random orientations. The crucial underlying physics of “locking” is that the ground state of the defect is two-fold degenerate—the Kramers’ degeneracy—and that transitions between these states do not occur at low temperature. The assumptions that the traps have a broad spectrum of energies, resulting in a wide range of characteristic trapping times, and that the processes are uncorrelated, lead to  $1/f$  flux noise. The fact that the noise amplitude scales only weakly with area—as the fourth root in the limit where the hole dimension is greater than the strip width—is consistent with experimental observations. The computed  $1/f$  noise magnitude agrees well with experimental values for a trap areal density of  $5 \times 10^{17} \text{ m}^{-2}$ . This is a reasonable value for unpassivated substrates that are exposed to atmospheric moisture. It is noteworthy that the two SQUIDS with the lowest  $1/f$  noise [2,3] were passivated. Our picture unifies the concepts of charge, critical current and flux noise: All three noise sources originate in the random filling and emptying of electron traps; flux noise, in addition, involves the concept of spin locking and the random direction of the magnetic moment associated with the trapped electron or hole.

Needless to say, there are unanswered questions. We do not know the kind or kinds of defects involved; most likely the defects in the superconductor oxide are different from those in  $\text{SiO}_2$ . The relatively uniform level of  $1/f$  flux noise among different devices—which implies a similarly uniform trap density—is also difficult to explain, beyond assuming that the oxide on silicon wafers is grown in a rather consistent way. One might hope that future

experiments will shed light on some of these issues, and ultimately lead to SQUIDs and qubits with lower levels of  $1/f$  flux noise.

We are grateful to Matt Copel and Sohrab Ismail-Beigi for helpful discussions. DDV is supported by the DTO through ARO contract number W911NF-04-C-0098; JC is supported by the Director, Office of Science, Office of Basic Energy Sciences, Materials Sciences and Engineering Division, of the U.S. Department of Energy under Contract No. DE-AC02-05CH11231.

## References

- [1] R.H. Koch *et al.*, J. Low Temp. Phys. **51**, 207 (1983).
- [2] V. Foglietti *et al.* , Appl. Phys. Lett. **49**, 1393 (1986).
- [3] C.D. Tesche *et al.*, IEEE Trans. Magn. **MAG-21**, 1032 (1985).
- [4] F.C. Wellstood, C. Urbina and J. Clarke, Appl. Phys. Lett. **50**, 772 (1987).
- [5] F. Yoshihara *et al.*, Phys. Rev. Lett. **97**, 167001 (2006).
- [6] C.T. Rogers and R.A. Buhrman, Phys. Rev. Lett. **53**, 1272 (1987).
- [7] R.T. Wakai and D.J. Van Harlingen, Phys. Rev. Lett. **58**, 1687 (1987).
- [8] J.M. Martinis *et al.*, Phys. Rev. B **67**, 094510 (2003).
- [9] M.J. Ferrari, *et al.*, J. Low Temp. Phys. **94**, 15 (1994).
- [10] E. Dantsker *et al.*, Appl. Phys. Lett. **69**, 4099 (1996).
- [11] P. Dutta and P.M. Horn, Rev. Mod. Phys. **53**, 497 (1981).
- [12] S. Machlup, J. Appl. Phys. **25**, 341 (1954).
- [13] D.L. Griscom, J. Non-Cryst. Solids **73**, 51 (1985).
- [14] J.M. Martinis *et al.*, Phys. Rev. Lett. **95**, 210503-1 (2005).
- [15] J. Schneider *et al.*, Appl. Phys. Lett. **74**, 200 (1999).
- [16] H.A. Kramers, Koninkl. Ned. Akad. Wetenschap., Proc. **33**, 959 (1930).
- [17] J.H. Van Vleck, Phys. Rev. **57**, 426 (1940).
- [18] E. Abrahams, Phys. Rev. **107**, 491 (1957).
- [19] C.P. Slichter, *Principles of Magnetic Resonance* (Springer, Berlin, 1990).
- [20] See, e.g., C. Kittel, *Introduction to Solid State Physics* (Wiley, New York, 1953), p.147.



[21] Strictly speaking, we should take into account two sets of defects for the area occupied by the loop: one in the substrate under the loop and the second from the oxide on the upper surface of superconductor.

[22] See [www.fastfieldsolvers.com](http://www.fastfieldsolvers.com).